

Synthesis and Characterization of Cyclotri- and Tetrasiloxanes with Pyrenyl Groups

Shin-ichi Kondo,* Marin Ito, Hiroki Ogawa, Wataru Fujiwara, and Hiroshi Katagiri

Cite This: *ACS Omega* 2022, 7, 44398–44406

Read Online

ACCESS |



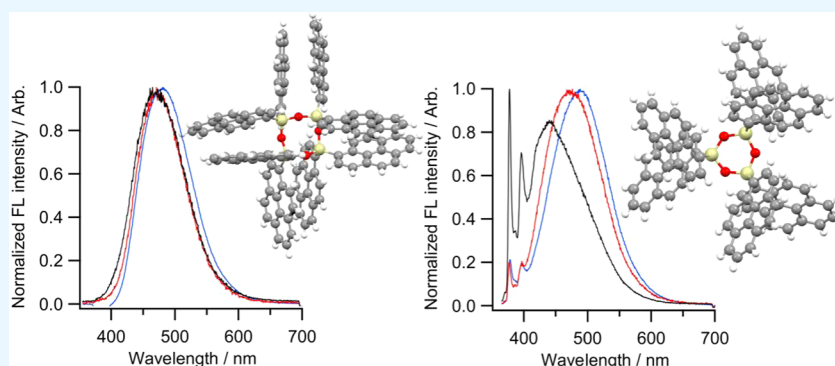
Metrics & More



Article Recommendations



Supporting Information



ABSTRACT: Cyclosiloxanes directly bearing polyaromatic groups on silicon atoms have scarcely been reported. Herein, hexa(1-pyrenyl)cyclotrisiloxane (**2**) and octa(1-pyrenyl)cyclotetrasiloxane (**3**) were successfully prepared from di(1-pyrenyl)silanediol (**1**) in the presence of a weak base such as tetraethylammonium acetate and triethylamine in MeCN. The structure of the cyclosiloxanes bearing multiple pyrenyl groups in the solid and solution states was evaluated by NMR, X-ray crystallography, and density functional theory (DFT) calculations. All pyrenyl groups of **2** were oriented outward, and no π - π stacking of adjacent pyrenyl groups was observed. However, all pairs of adjacent pyrenyl groups at 1- and 3-positions in **3** are oriented in the same direction and were π - π stacked with respect to each other. The UV-vis spectra of **2** and **3** in organic solvents showed a slight broadening of the peaks, as observed for typical pyrene derivatives. Interestingly, the fluorescence spectra of **2** showed small monomer and strong excimer emissions; however, those of **3** showed only a strong excimer emission in all solvents. Partially pyrenylated cyclotri- and tetrasiloxanes (compounds **4** and **5**) showed solvent-dependent monomer and excimer spectra as observed for di(1-pyrenyl)silane derivatives, implying that the excimer emissions of **2** and **3** arise from mainly geminal and vicinal pyrenyl groups, respectively.

INTRODUCTION

Cyclosiloxanes have widely been applied as starting materials of polysiloxanes,¹ ion transport,² and liquid crystals.³ The regulated structure of cyclosiloxanes should effectively provide the arrangement of functional groups on silicon atoms and the cyclosiloxane core is photochemically and electrically inert. Some cyclotetra- and trisiloxanes having substituted phenyl groups have been reported.⁴ A cyclotrisiloxane bearing the ferrocenyl group has also been prepared as a side product for the preparation of a silanediol having ferrocenyl groups.⁵ Recently, cyclosiloxanes having fluorescence moieties with appropriate linkers have been widely studied. Cyclotetrasiloxane having naphthyl,⁶ anthryl,⁷ pyrenyl,^{7–9} and BODIPY,¹⁰ with alkyl and alkenyl linkers have been prepared. However, cyclosiloxanes in which polycyclic aromatic hydrocarbons such as anthracene and pyrene are directly connected to silicon atoms have scarcely been reported. These compounds can be applied to functional materials due to the accumulation of the fluorescence functional groups in the cyclosiloxane core. Carbon nanocomposites¹¹ and self-assembly¹² with organic-

inorganic hybrid materials including cyclosiloxanes and silsesquioxanes have been in focus.

Cyclosiloxanes are generally prepared from the corresponding dichlorosilanes or silanediols in highly acidic or basic conditions, in which the Si-C bond of polycyclic aromatic hydrocarbon is labile in these conditions.¹³ Recently, highly effective condensation of phenylsilanol derivatives in liquid ammonia has been reported.¹⁴ During our study on anion recognition chemistry with silanols, we reported that 1,1,3,3-tetraphenyl-1,3-disiloxane-1,3-diols were smoothly condensed to form the corresponding hexaphenylcyclotrisiloxane and octaphenylcyclotetrasiloxane in the presence of acetate anion

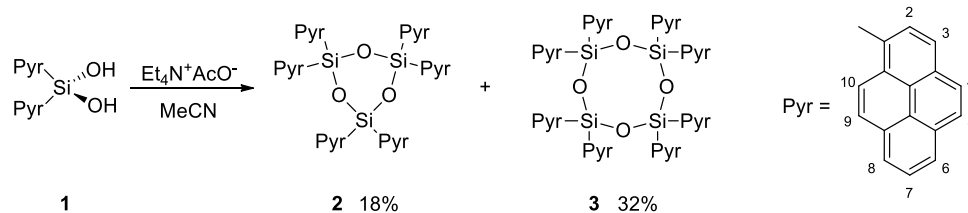
Received: September 20, 2022

Accepted: November 8, 2022

Published: November 17, 2022



Scheme 1. Synthesis of Cyclosiloxanes Bearing 1-Pyrenyl Groups



Scheme 2. Synthesis of Cyclosiloxanes Bearing Phenyl Groups and a Di(1-pyrenyl)silyl Unit

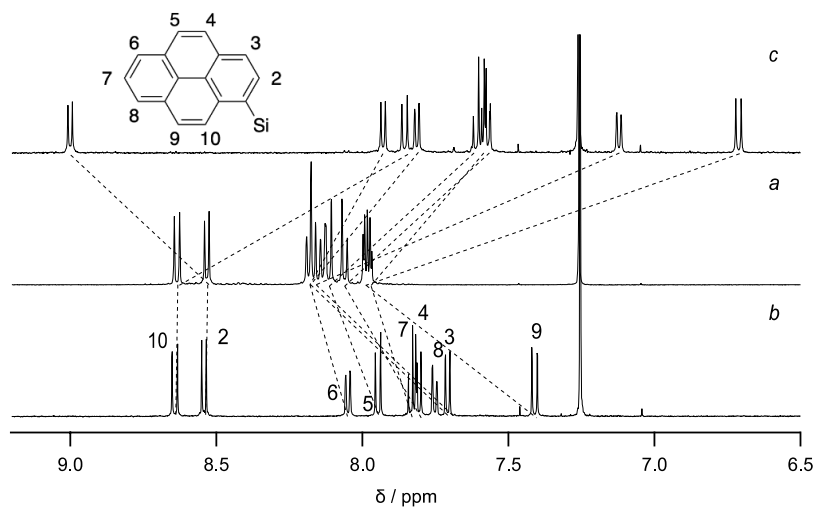
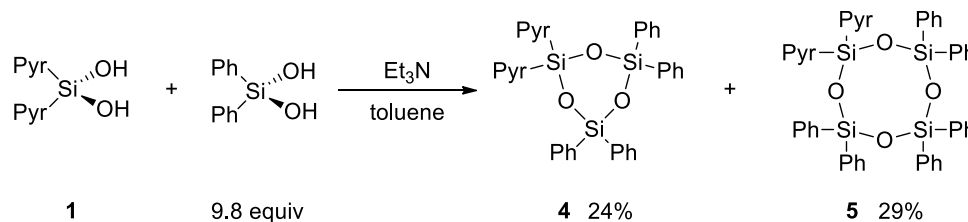


Figure 1. 500 MHz ^1H NMR spectra of **1** (a), **2** (b), and **3** (c) in CDCl_3 .

as a weak base in polar organic solvents such as acetonitrile within 1 h; however, the same reaction was dramatically slow (over 72 h) in apolar organic solvents such as chloroform.¹⁵ Acetate anion may activate the nucleophilicity of the Si–OH group as a general base and the polar pentavalent intermediate and/or the transition state on the substitution were stabilized in such polar organic solvents. We have also reported silanediol bearing two pyrenyl groups (**1**) as a novel fluorescent anion receptor.¹⁶ Monomer emission of pyrene is decreased and intramolecular excimer emission is increased upon the addition of anions such as acetate and dihydrogen phosphate. Therefore, favorable ratiometric fluorescence sensing can be achieved in these titrations. These results prompted us to prepare cyclosiloxanes bearing pyrenyl groups in the presence of a weak base by suppressing the cleavage of the Si–C bond of pyrenyl groups. We now report the synthesis and photophysical properties of cyclotrisiloxane **2** and cyclotetrasiloxane **3** bearing six and eight pyrenyl groups, respectively, starting from di(1-pyrenyl)silaneediol in acetonitrile in the presence of a weak base such as tetraethylammonium acetate and triethylamine (Scheme 1).

Synthesis. Hexa(1-pyrenyl)cyclotrisiloxane (**2**) and octa(1-pyrenyl)cyclotetrasiloxane (**3**) were successfully prepared from

di(1-pyrenyl)silaneediol (**1**) in the presence of tetraethylammonium acetate in MeCN at 60 °C in 18 and 32% yield, respectively. No reaction proceeded at room temperature (rt) and decomposition of **1** was observed at higher temperatures (over 75 °C) to give pyrene by the cleavage of the Si–C bond determined by thin-layer chromatography (TLC) and NMR analyses. The reaction of **1** in the presence of strong acid and base, such as HCl and NaOH, respectively, gave also pyrene by the scission of the Si–C bond. Interestingly, the reaction of **1** with the addition of a weak acid such as pyridinium *p*-toluenesulfonate also afforded pyrene. However, the reaction of **1** in the presence of triethylamine in MeCN gave **2** and **3** in 10 and 10% yields, respectively, at 60 °C. Surprisingly, the reaction is highly dependent on the solvent. In dimethylsulfoxide (DMSO) and tetrahydrofuran (THF), no product was observed in the same condition. Reaction in chloroform for 3 h afforded **2** and **3** in 14 and 10% yields, respectively, and reaction in toluene for 3 h gave **2** and **3** in 17 and 6%, yields, respectively. These results suggest that the formation of cyclotri- and tetrasiloxane from silaneediol with weak bases is quite a unique and significantly useful method. These cyclosiloxanes were easily separated by silica gel column chromatography from the reaction mixture; however, the

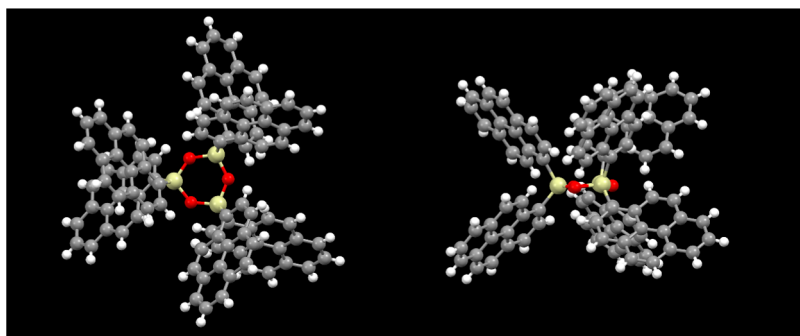


Figure 2. X-ray crystal structure of **2**.

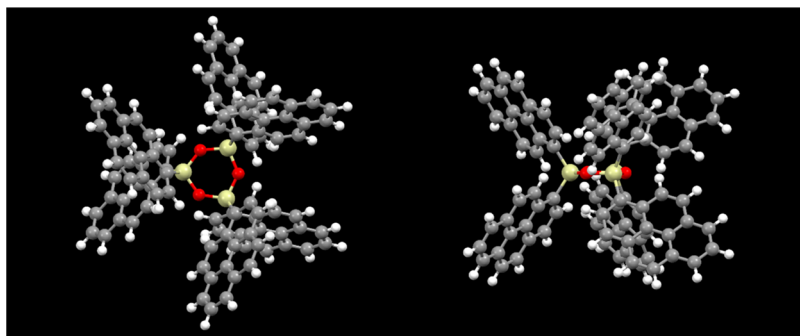


Figure 3. Optimized structure of **2** by DFT calculation (B3LYP/6-31G(d) level of theory).

purified solids after evaporation were less soluble in common organic solvents. The products were fully characterized by NMR, field desorption mass spectroscopy (FD-MS), and electrospray ionization (ESI-MS) as discussed below.

To evaluate the photophysical properties, particularly the fluorescence characters of **2** and **3**, cyclosiloxanes having diphenylsilyl groups and one di(1-pyrenyl)silyl unit, 1,1,3,3-tetraphenyl-5,5-di(1-pyrenyl)cyclotrisiloxane (**4**), and 1,1,3,3,5,5-hexaphenyl-7,7-di(1-pyrenyl)cyclotetrasiloxane (**5**) were also prepared by the condensation of di(1-pyrenyl)silane diol in the presence of excess diphenylsilane diol in toluene with triethylamine as a base (Scheme 2). The products were successfully isolated by column chromatography on silica gel. The structures of **4** and **5** were also confirmed by NMR techniques and MS.

MS and NMR. Mass spectrometry clearly identified isolated **2** and **3**. FD-MS of **2** and **3** gave m/z 1338.34 and 1784.45, respectively. These values are in good agreement with the theoretical m/z of $[M]^+$. High-resolution mass spectrometry (HRMS) by ESI-MS also gave similar results.

Proton NMR spectra of **2**, **3**, and the starting material **1** are shown in Figure 1. All pyrene signals appeared separately, suggesting that all pyrenyl groups freely rotate and are magnetically identical at least in the NMR timescale. All signals were fully assigned with the aid of ^{13}C NMR and two-dimensional (2D) NMR techniques, such as correlation spectroscopy (COSY), heteronuclear multiple quantum coherence (HMQC), and heteronuclear multiple bond correlation (HMBC). In the case of **2**, 2- and 10-CH were almost identical positions for the original **1**, respectively. However, other C–H protons showed a slightly upfield shift compared with those of **1**. In the case of **3**, only 2-CH protons were significantly downfield shifted, but other all protons including 10-CH showed an upfield shift. Shielding and

deshielding of neighboring pyrenyl groups should cause these NMR shifts. These results suggest different structures of **2** and **3** in the ground state.

The chemical shift of siloxane, particularly cyclosiloxanes on ^{29}Si NMR reflects their structural information.¹⁷ The ^{29}Si NMR of cyclosiloxanes **2** and **3** gave a singlet peak at -29.4 and -37.0 ppm, respectively. The ^{29}Si NMR signals for analogous hexaphenylcyclotrisiloxane¹⁸ and octaphenylcyclotetrasiloxane¹⁹ were observed at -37.0 and -42.8 ppm, respectively, indicating that the ^{29}Si NMR signals of **2** and **3** are slightly downfield shifted compared with the corresponding phenyl analogues, which may due to the larger ring current of the pyrenyl groups.

X-ray Structures and Density Functional Theory (DFT) Calculations. The single crystals of **2** and **3** were obtained by recrystallization from chloroform–hexane. The X-ray structure of **2** as depicted in Figure 2 shows a trigonal $R\bar{3}$ space group and that of compound **2** shows a D_3 symmetry. The siloxane ring is almost planar with mean deviations of 0.060 Å for both silicon and oxygen atoms. All of the pyrenyl groups in the same plane are positioned in the same propeller-like direction, and the pyrenyl groups in another plane are positioned in opposite directions. The angle between two pyrenyl groups on one silicon atom is 86.48° . To clarify the structure in the solution, DFT calculations of **2** were performed at the B3LYP/6-31G(d) level of theory. The energy-optimized structures of cyclosiloxanes **2** are depicted in Figure 3. The structure of **2** predicted by the DFT calculation also shows a D_3 symmetry and the orientation and angles of the pyrenyl groups are essentially identical to the structure obtained from the X-ray crystallography, strongly suggesting the structure in solution is almost similar to the solid state. From the X-ray structures of hexaphenylcyclotrisiloxane (**6**),²⁰

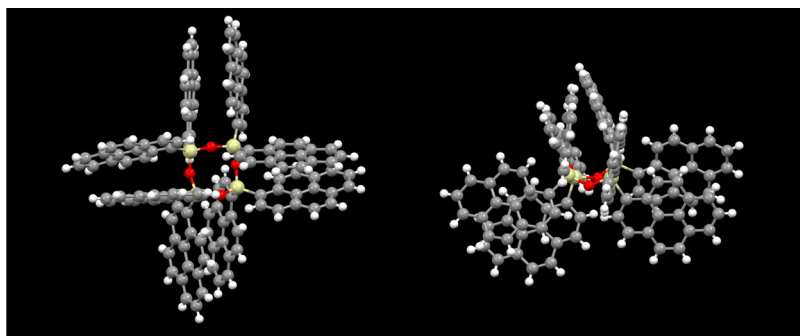


Figure 4. X-ray crystal structure of 3.

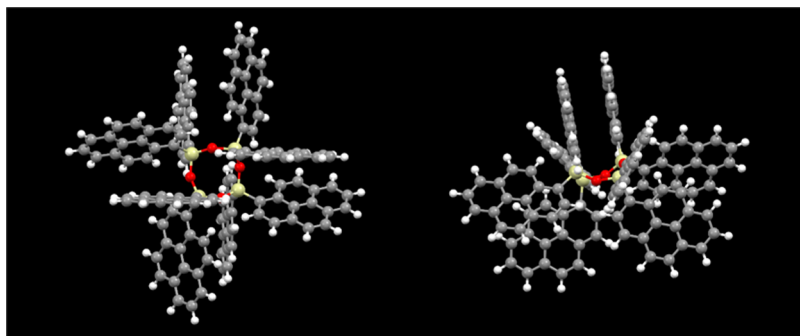


Figure 5. Optimized structure of 3 by DFT calculation (B3LYP/6-31G(d) level of theory).

all phenyl groups were oriented outward and no π - π stacking of adjacent phenyl groups was observed in the structure of 2.

The X-ray structure of 3 is illustrated in Figure 4. The siloxane ring is not a planar structure with mean deviations of 0.300–0.286 Å for silicon atoms. Larger mean deviations are observed in 0.566–0.580 Å for oxygen atoms, and two opposite oxygens are located on the upper side of the mean plane and the remaining opposite oxygens are located lower side of the mean plane. Interestingly, all pairs of adjacent pyrenyl groups at 1- and 3-positions are oriented in the same direction and π - π stacked with each other. The optimized structure by the DFT calculation (B3LYP/6-31G(d) level of theory (Figure 5) shows overall similarity but the π -surfaces of the pyrenyl groups are slightly tilted to the stacked π -surfaces of the pyrenyl groups. The π - π stacking may be the origin of the upfield shift of the pyrenyl C–H protons except for 2-CH of the pyrenyl groups in the ^1H NMR spectrum. Importantly, in the solid-state structure of octaphenylcyclotetrasiloxane (7),²¹ no π - π stacking of adjacent phenyl groups at 1- and 3-positions of cyclotetrasiloxane was observed, implying strong π - π stacking of the pyrenyl groups of 3 due to the larger π -surface.

These structural differences may lead to the difference in the magnetic environment of pyrenes in 2 and 3, resulting in the large chemical shift changes of 2 and 3 as discussed above.

IR Spectra of 2 and 3. The strong Si–O–Si asymmetric stretching vibrations of cyclotetrasiloxanes 2 and 3 were observed at 993 and 985 cm^{-1} on the IR spectra, respectively. In addition, the characteristic peaks at 1036 and 1034 cm^{-1} for 2 and 3 were assigned to the stretching vibrations of Si–C, respectively.

UV–vis and Fluorescence Spectra of 2 and 3. West and co-workers reported that fluorescence cyclotri- and tetrasiloxanes contain silafluorene²² and silole²³ skeletons.

Fluorescent properties of a cyclotetrasiloxane having naphthalene diimides via decamethylene spacer²⁴ and cyclotetrasiloxanes bearing 9-anthrylethenyl and 1-pyrenylethenyl groups^{7,8} (via ethenyl spacers) have also been reported. Fluorescence and sensing ability of cyclotetrasiloxane-based porous polymers with pyrene, tetraphenylethene, and spirobifluorene were also described by Wang et al.²⁵ Nemoto et al. reported that a siloxane-bridged cyclic dimer with 1,6-pyrenylene moieties showed strong excimer emission due to the parallel arrangement of two pyrenyl groups from the restricted cyclophane structure.²⁶ However, UV–vis and fluorescence spectra of cyclotetrasiloxanes bearing polyaromatic substituents on silicone atoms have never been reported. The cyclotetrasiloxanes 2 and 3 have many pyrenyl groups; therefore, the photophysical properties of these compounds are quite interesting.

UV–vis spectra of cyclotrisiloxane 2 in various solvents, like cyclohexane, chloroform, acetonitrile, and dimethylsulfoxide, were typical of pyrene derivatives. The absorbance maxima are summarized in Table 1. The UV–vis spectra of 1,1,3,3-tetraphenyl-5,5-di(1-pyrenyl)cyclotrisiloxane 4 (Figure 6) also

Table 1. Photophysical Properties of Cyclotetrasiloxanes Bearing 1-Pyrenyl Groups

compound	solvent	λ_{max} (nm)	λ_{em} (nm)	Φ_{F}
2	cyclohexane	334.5, 351.0	445.5	0.254
2	CHCl_3	336.0, 352.5	440.0	0.173
2	MeCN	334.0, 350.5	473.0	0.056
2	DMSO	336.5, 352.5	489.0	0.118
3	cyclohexane	336.0, 352.5	467.2	0.235
3	CHCl_3	337.0, 353.5	471.4	0.137
3	MeCN	335.5, 352.0	474.2	0.072
3	DMSO	337.5, 353.5	481.6	0.210

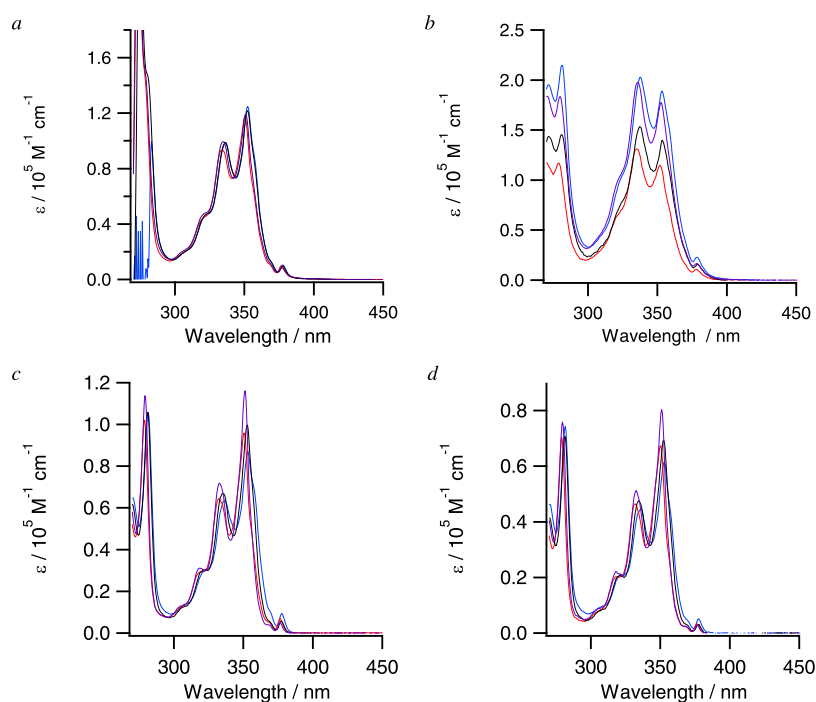


Figure 6. UV–vis spectra of (a) **2**, (b) **3**, (c) **4**, and (d) **5** in cyclohexane (purple line), CHCl_3 (black line), MeCN (red line), and DMSO (blue line).

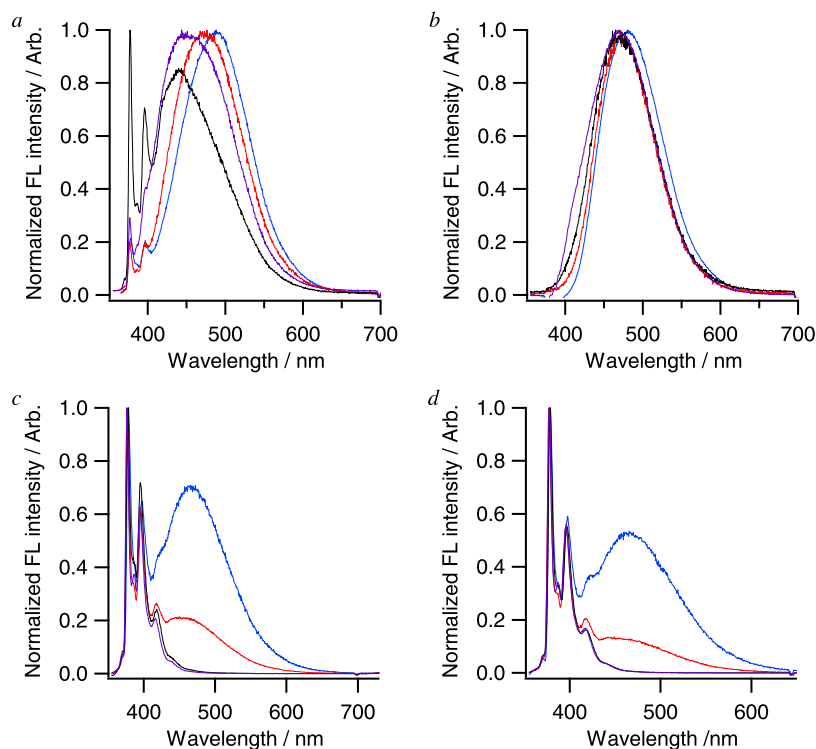


Figure 7. Fluorescence spectra of (a) **2**, (b) **3**, (c) **4**, and (d) **5** in cyclohexane (purple line), CHCl_3 (black line), MeCN (red line), and DMSO (blue line).

showed similar spectra for **2**, suggesting that the interaction of pyrenyl groups in the ground state is weak or less significant. The UV–vis spectra of **3** are slightly broad compared with those of the pyrene derivatives such as 1,1,3,3,5,5-hexaphenyl-7,7-di(1-pyrenyl)cyclotetrasiloxane **5**, suggesting a weak interaction of vicinal pyrenyl groups of **3** in the ground state.

In the fluorescence spectra, **2** showed small monomer and strong excimer emission as shown in Figure 7 and Table 1. The red-shift of the emission maxima of excimer of **2** depending on the solvent polarity ($\lambda_{\text{em}} = 440$ nm in CHCl_3 and 489 nm in DMSO) was observed. However, **3** showed only strong excimer emission in all solvents and a smaller ($\lambda_{\text{em}} = 470$ nm in CHCl_3 and 481 nm in DMSO) red-shift was observed.

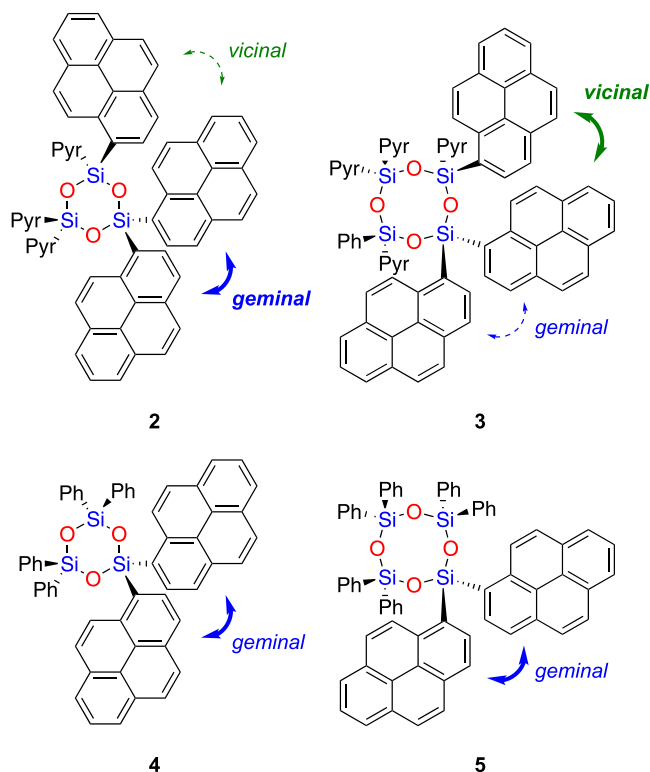
The spectral shape is not dependent on the concentrations of **2** and **3**, implying an intramolecular excimer rather than an intermolecular one.

The fluorescence quantum yields (Φ_F) of cyclosiloxanes **2** and **3** in cyclohexane, chloroform, acetonitrile, and dimethylsulfoxide were determined with respect to quinine sulfate in 0.1 mol dm⁻³ as a reference, and the results are summarized in Table 1. Moderate quantum yields of both **2** and **3** were observed in cyclohexane (0.254 and 0.210, respectively), although the smallest quantum yields were shown in acetonitrile (0.056 and 0.072).

Ervithayasuporn et al. reported cyclotetrasiloxane bearing four 1-pyrenyl groups via ethenyl spacer.⁷ The cyclotetrasiloxane showed both monomer and excimer emissions in various organic solvents such as toluene, THF, DMF, and DMSO. Lin et al. reported that the same cyclotetrasiloxane having (1-pyrenyl)ethenyl groups showed only monomer emission in dichloromethane.⁸ Interestingly, cyclotetrasiloxane **3** showed no monomer and strong excimer emissions, suggesting an effective intramolecular overlap of the pyrenyl groups in the excited state due to the rigidity of the direct connection of the pyrenyl groups with silicon atoms. Therefore, cyclosiloxanes **2** and **3** can be used as a fluorescence material with the large Stokes shift.

We have recently reported that di(1-pyrenyl)silanediol **1** and dimethyldi(1-pyrenyl)silane show unique solvent-dependent intramolecular excimer-like emissions. Only structured monomer emission at around 370 nm was observed in apolar organic solvents such as chloroform; however, broad emission at a longer wavelength around 470 nm was prominent in polar organic solvents such as acetonitrile, DMSO, and aqueous solutions.²⁷ These findings suggest that there are two possible causes of an excimer-like emission in the longer-wavelength region for the cyclosiloxanes. One is that the two pyrenyl groups is connected to one silicone atom to form a *geminal* excimer as dipyrenylsilane derivatives. The other is that the pyrenyl groups on neighboring silicon atoms form a *vicinal* excimer. To ascertain these two possibilities, we prepared cyclotri- and tetrasiloxanes having both pyrenyl and phenyl groups (cyclotrisiloxane **4** and cyclotetrasiloxane **5**). In these cases, an excimer by *geminal* pyrenyl groups can be formed, but the *vicinal* excimer formation should be ignored as depicted in Scheme 3. Partially pyrene-substituted cyclotrisiloxane **4** showed similar broad fluorescence spectra to all pyrene-substituted cyclosiloxane **2** in the excimer region in polar organic solvents. However, sufficient excimer-like emission of **2** can be observed even in the apolar chloroform. These results suggest that the excimer-like emission of **2** originated mainly from the *geminal* pyrenyl groups and a small contribution of the *vicinal* pyrenyl groups, which are separated by the demand of the cyclotrisiloxane structure. Surprisingly, partially pyrene-substituted **5** showed monomeric fluorescence in apolar solvent chloroform and monomer and excimer emissions in the polar solvent DMSO. These spectra are significantly different from those of all pyrenyl **3**. The characteristic spectral changes on solvent are similar to dipyrenylsilane derivatives as previously reported.²⁷ Therefore, the emission of all pyrenyl **3** observed at a longer wavelength mainly arises from the *vicinal* pyrenyl groups connected to the neighboring silicon atoms. Of course, excimer-like emission from the *geminal* pyrenyl groups is also observed; however, the contribution of the emission might be small.

Scheme 3. Origins of the Emissions of **2**–**5**



Cyclosiloxanes **2** and **3** can be applied as functional materials due to the congested pyrenyl units in the cyclosiloxane skeleton. For example, the cyclosiloxanes and fullerene C₆₀ complex could be formed because of the interaction of electron-rich pyrenyl groups and electron-deficient C₆₀ as observed for octaphenylcyclotetrasiloxane with C₆₀.²⁸ The multiple pyrenyl groups of the cyclosiloxanes **2** and **3** might interact with nitro aromatic compounds due to the electron deficiency.⁸ Therefore, such explosive compounds can be detected. Ervithayasuporn et al. reported that cyclotetrasiloxane bearing (1-pyrenyl)ethenyl groups showed fluorescence response to anions such as F⁻, CN⁻, and PO₄³⁻;⁷ therefore, anion recognition by cyclosiloxanes **2** and **3** is another candidate for application.

Conclusions. In summary, we have successfully prepared **2** and **3** from dipyrenylsilanediol with a weak base such as acetate anion and triethylamine in moderate yield. The structure was fully characterized by mass spectrometry, NMR, X-ray, and UV–vis and fluorescence spectroscopies. Both cyclosiloxanes **2** and **3** showed similar excimer emissions at about 470 nm mainly due to the *geminal* and *vicinal* pyrenyl groups, respectively. The present synthetic procedure for the preparation of cyclosiloxane directly bearing aromatic groups can be employed for preparing cyclosiloxanes with substituted aromatic moieties. Applications of cyclosiloxanes **2** and **3** including recognition of electron-deficient compounds and anions are in progress in our laboratory.

EXPERIMENTAL SECTION

General. All reagents used were of analytical grade. Acetonitrile was distilled over calcium hydride. NMR spectra were measured on a JEOL ECA-500 (500 MHz) spectrometer. UV–vis spectra were recorded on a Shimadzu UV-2500PC spectrometer with a thermal regulator (± 0.5 °C). Fluorescence

spectra were recorded on a Hitachi F-7000 spectrofluorometer. Fourier transform infrared spectroscopy (FTIR) spectra were recorded on a Thermo Fisher Scientific Nicolet 6700 spectrometer. FD-MS was measured on JEOL AccuTOF 4G GC. HRMS were measured in CHCl₃/MeOH = 3:1 at 150–200 °C on ABI Sciex TripleTOF 4600. Column chromatography was performed using Silica Gel 60N from Kanto Reagents. Melting points were determined with a Yanagimoto MP-J3 micro melting point apparatus and are uncorrected. Di(1-pyrenyl)silanediol was prepared according to the literature.¹⁶

Synthesis of Hexa(1-pyrenyl)cyclotrisiloxane and Octa(1-pyrenyl)cyclotetrasiloxane. A mixture of di(1-pyrenyl)silanediol (87 mg, 0.19 mmol) and tetramethylammonium acetate (74 mg, 0.25 mmol) in 10 mL of acetonitrile was stirred at 60 °C under an argon atmosphere overnight. The mixture was evaporated under reduced pressure and the residue was chromatographed on silica gel (CHCl₃/cyclohexane = 1:1 as an eluent) to give hexa(1-pyrenyl)cyclotrisiloxane (15 mg, 18%) as a colorless solid and octa(1-pyrenyl)cyclotetrasiloxane (27 mg, 32%) as a pale yellow solid.

Hexa(1-pyrenyl)cyclotrisiloxane. ¹H NMR (500 MHz, CDCl₃) δ 8.58 (d, 6H, *J* = 9.2 Hz), 8.48 (d, 6H, *J* = 7.5 Hz), 7.97 (d, 6H, *J* = 7.5 Hz), 7.87 (d, 6H, *J* = 9.2 Hz), 7.75 (t, 6H, *J* = 7.5 Hz), 7.73 (d, 6H, *J* = 9.2 Hz), 7.66 (d, 6H, *J* = 7.5 Hz), 7.64 (d, 6H, *J* = 7.5 Hz), 7.33 (d, 6H, *J* = 9.2 Hz). ¹³C NMR (126 MHz, CDCl₃) δ 135.9, 133.3, 133.0, 130.9, 130.4, 130.2, 128.4, 127.8, 127.4, 127.1, 125.6, 125.2, 125.1, 124.4, 124.3, 124.1. ²⁹Si NMR (99 MHz, CDCl₃) δ -29.4. IR (ATR) 1036 (ν Si–C), 993 (ν_{as} Si–O–Si) cm⁻¹. FD-MS: Calcd for C₉₆H₅₄O₃Si₃ [M]⁺, 1338.34. Found 1338.57. HRMS (ESI, positive mode): Calcd for C₉₆H₅₅O₃Si₃ [M + H]⁺, 1339.3454. Found 1339.3674.

Octa(1-pyrenyl)cyclotetrasiloxane. ¹H NMR (500 MHz, CDCl₃) δ 8.90 (d, 8H, *J* = 7.5 Hz), 7.83 (d, 8H, *J* = 9.2 Hz), 7.82 (d, 8H, *J* = 7.5 Hz), 7.74 (d, 8H, *J* = 7.5 Hz), 7.54 (d, 8H, *J* = 9.2 Hz), 7.51 (t, 8H, *J* = 7.5 Hz), 7.50 (d, 8H, *J* = 9.2 Hz), 7.08 (d, 8H, 7.5 Hz), 6.67 (d, 8H, *J* = 9.2 Hz). ¹³C NMR (126 MHz, CDCl₃) δ 135.2, 132.4, 132.2, 130.4, 130.4, 129.9, 127.8, 126.7, 126.5, 126.4, 124.9, 124.6, 124.5, 123.6, 123.5, 123.4. ²⁹Si NMR (99 MHz, CDCl₃) δ -37.0. IR (ATR) 1034 (ν Si–C), 985 (ν_{as} Si–O–Si) cm⁻¹. FD-MS: Calcd for C₁₂₈H₇₂O₄Si₄ [M]⁺, 1784.45. Found 1784.79. HRMS (ESI, positive mode): Calcd for C₁₂₈H₇₃O₄Si₄ [M + H]⁺, 1785.4580. Found 1785.5020.

Synthesis of 1,1,3,3-Tetraphenyl-5,5-di(1-pyrenyl)cyclotrisiloxane and 1,1,3,3,5,5-Hexaphenyl-7,7-di(1-pyrenyl)cyclotetrasiloxane. A mixture of di(1-pyrenyl)silanediol (51 mg, 0.11 mmol), diphenylsilanediol (233 mg, 1.08 mmol), and triethylamine (3.3 mL, 23.6 mmol) in 20 mL of toluene was stirred at 60 °C under an argon atmosphere for 3 h. The mixture was evaporated under reduced pressure and the residue was chromatographed on silica gel (CHCl₃/hexane = 1:2 as an eluent) to give 1,1,3,3-tetraphenyl-5,5-di(1-pyrenyl)cyclotrisiloxane (22 mg, 24%) and 1,1,3,3,5,5-hexaphenyl-7,7-di(1-pyrenyl)cyclotetrasiloxane (33 mg, 29%) as pale yellow solids.

1,1,3,3-Tetraphenyl-5,5-di(1-pyrenyl)cyclotrisiloxane. ¹H NMR (500 MHz, CDCl₃, 298 K) δ 8.59 (d, 2H, *J* = 9.5 Hz), 8.42 (d, 2H, *J* = 7.5 Hz), 8.14 (d, 2H, *J* = 7.0 Hz), 8.08 (d, 2H, *J* = 9.0 Hz), 8.07 (d, 2H, *J* = 6.0 Hz), 8.02 (d, 2H, *J* = 7.5 Hz), 8.00 (d, 2H, *J* = 8.5 Hz), 7.94 (t, 2H, *J* = 7.75 Hz),

7.74 (d, 2H, *J* = 9.5 Hz), 7.63 (d, 8H, *J* = 7.0 Hz), 7.33 (t, 4H, *J* = 7.5 Hz), 7.19 (t, 8H, *J* = 7.5 Hz). ¹³C NMR (126 MHz, CDCl₃, 298 K) δ 135.9, 134.5, 133.8, 133.6, 133.1, 131.1, 130.6, 130.4, 130.2, 128.5, 128.1, 127.7, 127.5, 127.4, 125.7, 125.4, 125.2, 124.6, 124.5, 124.1. ²⁹Si NMR (99 MHz, CDCl₃) δ -30.6, -33.4. HRMS (FD, positive mode): Calcd for C₅₆H₃₈O₃Si₃ [M]⁺, 842.2129. Found 842.2114.

1,1,3,3,5,5-Hexaphenyl-7,7-di(1-pyrenyl)cyclotetrasiloxane. ¹H NMR (500 MHz, CDCl₃) δ 8.40 (d, 2H, *J* = 7.0 Hz), 8.40 (d, 2H, *J* = 9.5 Hz), 8.14 (d, 2H, *J* = 7.0 Hz), 8.09 (d, 2H, *J* = 9.0 Hz), 8.02 (d, 2H, *J* = 8.5 Hz), 8.00 (d, 2H, *J* = 8.0 Hz), 7.94 (d, 2H, *J* = 7.5 Hz), 7.93 (t, 2H, *J* = 7.8 Hz), 7.51 (d, 2H, *J* = 6.5 Hz), 7.51 (d, 4H, *J* = 9.5 Hz), 7.40 (d, 8H, *J* = 6.0 Hz), 7.33 (t, 2H, *J* = 7.5 Hz), 7.15 (t, 4H, *J* = 7.8 Hz), 7.14 (t, 4H, *J* = 7.0 Hz), 6.94 (t, 8H, *J* = 7.8 Hz). ¹³C NMR (126 MHz, CDCl₃) δ 135.8, 134.5, 134.4, 134.3, 134.1, 133.2, 133.0, 131.0, 130.7, 130.6, 130.0, 129.8, 128.3, 127.9, 127.6, 127.4, 127.3, 125.6, 125.2, 125.0, 124.6, 124.4, 124.2. ²⁹Si NMR (99 MHz, CDCl₃) δ -39.3, -42.5. HRMS (FD, positive mode): Calcd for C₆₈H₄₈O₄Si₄ [M]⁺, 1040.2630. Found 1040.2629.

Single-Crystal X-ray Diffraction. Crystallographic data for **2** and **3** are summarized in Table 2.

Table 2. Crystal Data for Cyclosiloxanes **2** and **3**

	2	3
empirical formula	C ₉₆ H ₅₄ O ₃ Si ₃	C ₁₃₈ H ₉₀ Cl ₁₂ O ₄ Si ₄
MW	1463.94	2349.85
<i>T</i> (K)	93	150
<i>λ</i> (Mo <i>Kα</i>) (Å)	0.71073	0.71073
space group	R $\bar{3}$ (#148)	P2/ <i>n</i> (#13)
<i>a</i> (Å)	17.9776(2)	21.3909(10)
<i>b</i> (Å)	17.9776(2)	11.3135(5)
<i>c</i> (Å)	39.9810(6)	22.5844(11)
<i>α</i> (deg)	90	90
<i>β</i> (deg)	90	90.376(4)
<i>γ</i> (deg)	120	90
<i>V</i> (Å ³)	11190.5	5465.4(4)
<i>Z</i>	6	2
<i>D</i> _{calcd} (g cm ⁻³)	1.303	1.309
reflections collected	4891	9940
independent reflections	4252	4700
GOF	1.104	1.950
<i>R</i> ₁ , <i>wR</i> ₂ (<i>I</i> > 2σ(<i>I</i>))	0.0785, 0.2277	0.1448, 0.3720
<i>R</i> ₁ , <i>wR</i> ₂ , all data	0.0900, 0.2432	0.2371, 0.4347
CCDC number	2206726	2206725

Crystals of **2** were obtained by the vapor diffusion of hexane into a solution of **2** in CHCl₃. Data collection was carried out at 93 K on a Rigaku Saturn-70 CCD detector with graphite-monochromated Mo *Kα* radiation (*λ* = 0.71073 Å). The structure was solved by the direct method (SHELXS-2014²⁹) and refined by full-matrix least squares methods on *F*² using SHELXL-2014.³⁰ Nonhydrogen atoms were refined anisotropically. Diffused solvent molecules were treated with the Squeeze program.

Crystals of **3** were also obtained by vapor diffusion of hexane into a solution of **3** in CHCl₃. Data collection was carried out at 100 K on a Rigaku Saturn-70 CCD detector with graphite-monochromated Mo *Kα* radiation (*λ* = 0.71073 Å). The structure was solved by the direct method (SHELXS-2014) and refined by full-matrix least squares methods on *F*² using

SHELXL-2018.³⁰ Nonhydrogen atoms were refined anisotropically.

Crystallographic data for the structures in this paper have been deposited with the Cambridge Crystallographic Data Centre as supplementary publication numbers shown in Table 1.

DFT Calculations. Conformational analysis of **2** and **3** was performed by molecular mechanics calculation with MMFF force field and fifty initial geometries were generated by a Spartan '14 program. All of the geometries were optimized by semiempirical molecular orbital calculations using PM6 Hamiltonian. Ten energetically lower independent geometries were optimized with the B3LYP/6-31G(d) level of theory in vacuo using Gaussian 16 Rev A.03.³¹ The structures with the lowest energy are shown in Figures 3 and 4.

Determination of Quantum Yields. Fluorescence quantum yields were determined from the derived fluorescence spectrum of each species using quinine sulfate as standard ($\Phi_{\text{QS}} = 0.546$ in $0.5 \text{ mol dm}^{-3} \text{ H}_2\text{SO}_4$ at 298 K) and were corrected for solvent refractive index. Into an appropriate solvent (3 mL) in a quartz cell, an aliquot of the stock solution of the cyclosiloxane was added with a microsyringe and UV–vis and fluorescence spectra (excited at 320 nm) were measured at $298 \pm 0.5 \text{ K}$. The process was repeated at least four additional times. The integrated fluorescence intensities of the probes were plotted against the UV–vis absorbance at each concentration to give the slope F/A , in which F and A are the integrated fluorescence intensity and the absorbance of the cyclosiloxanes, respectively. The same procedure was performed for quinine sulfate in $0.5 \text{ mol dm}^{-3} \text{ H}_2\text{SO}_4$ at $298 \pm 0.5 \text{ K}$ to give $F_{\text{QS}}/A_{\text{QS}}$, in which F_{QS} and A_{QS} are the integrated fluorescence intensity and the absorbance of the quinine sulfate, respectively. The quantum yield of the probes Φ_{F} was calculated according to the equation

$$\Phi_{\text{F}} = \Phi_{\text{QS}} \frac{F/A}{F_{\text{QS}}/A_{\text{QS}}} \left(\frac{n}{n_{\text{QS}}} \right)^2$$

where n and n_{QS} are the refractive indexes of the measured solvent and $0.5 \text{ mol dm}^{-3} \text{ H}_2\text{SO}_4$, respectively.

■ ASSOCIATED CONTENT

SI Supporting Information

The Supporting Information is available free of charge at <https://pubs.acs.org/doi/10.1021/acsomega.2c06076>.

Synthesis, ¹H NMR, ¹³C NMR spectra of compounds, and Cartesian coordinates of the optimized structures (PDF)

Accession Codes

CCDC 2206725–2206726 contains the supplementary crystallographic data for this paper. Copies of the data can be obtained, free of charge, on application to CCDC, 12 Union Road, Cambridge CB2 1EZ, UK [fax: +44(0)-1223-336033 or e-mail: deposit@ccdc.cam.ac.uk].

■ AUTHOR INFORMATION

Corresponding Author

Shin-ichi Kondo – Department of Chemistry, Faculty of Science, Yamagata University, Yamagata-shi, Yamagata 990-8560, Japan; orcid.org/0000-0003-1518-5274; Email: kondo@sci.kj.yamagata-u.ac.jp

Authors

Marin Ito – Department of Chemistry, Faculty of Science, Yamagata University, Yamagata-shi, Yamagata 990-8560, Japan

Hiroki Ogawa – Department of Chemistry, Faculty of Science, Yamagata University, Yamagata-shi, Yamagata 990-8560, Japan

Wataru Fujiwara – Graduate School of Science and Engineering, Yamagata University, Yonezawa, Yamagata 992-8510, Japan

Hiroshi Katagiri – Graduate School of Science and Engineering, Yamagata University, Yonezawa, Yamagata 992-8510, Japan; orcid.org/0000-0003-4100-9995

Complete contact information is available at:

<https://pubs.acs.org/10.1021/acsomega.2c06076>

Notes

The authors declare no competing financial interest.

■ ACKNOWLEDGMENTS

The authors would like to thank JSPS KAKENHI Grant Number 21K05032, professors Tatsuya Nabeshima and Masaki Yamamura from the University of Tsukuba for the measurements of HRMS (ESI) of the compounds. They also thank professors Masafumi Unno and Nobuhiro Takeda, Gunma University, for the measurements of FD-MS.

■ REFERENCES

- (1) Clarson, S. J.; Semlyen, J. A. *Siloxane Polymers*; Prentice Hall, 1993.
- (2) Zhang, Z.; Lyons, L. J.; Jin, J. J.; Amine, K.; West, K. A. Synthesis and ionic conductivity of cyclosiloxanes with ethyleneoxy-containing substituents. *Chem. Mater.* **2005**, *17*, 5646–5650.
- (3) (a) Lacey, D.; Mann, E. T. Preparation and evaluation of novel ferroelectric liquid crystalline cyclic siloxane tetramer. *Liq. Cryst.* **2003**, *30*, 1159–1170. (b) Liu, L.-M.; Zhang, B.-Y.; He, X.-Z.; Cheng, C.-S. Cyclic versus linear siloxane liquid crystalline oligomers: phase behaviour. *Liq. Cryst.* **2004**, *31*, 781–786.
- (4) (a) Schott, G.; Berge, H. S., II. Condensation products of bis(p-chlorophenyl)silanediol. *Z. Anorg. Allg. Chem.* **1959**, *297*, 44–47. (b) Uhle, K. Thin-layer chromatographic studies of silanols, siloxanes, and silanes. *Z. Chem.* **1967**, *7*, 236–237. (c) Ishikawa, N.; Kuroda, K. Formation of octaarylcyloctetrasiloxanes by reaction of diaryldifluoro-silanes with alkylamines. *Nippon Kagaku Kaishi* **1969**, *90*, 416–419. (d) Tanasova, M.; Chirakadze, G. Synthesis of colored oligomeric cyclosiloxanes. *Izv. Akad. Nauk Gruz. SSR, Ser. Khim.* **2001**, *27*, 240–242.
- (5) Bruña, S.; Garrido-Castro, A. F.; Perles, J.; Montero-Campillo, M. M.; M6, O.; Kaifer, A. E.; Cuadrado, I. Multi-ferrocene-containing silanols as redox-active anion receptors. *Organometallics* **2016**, *35*, 3507–3519.
- (6) Belova, A. S.; Kononevich, Y. N.; Sazhnikov, V. A.; Safonov, A. A.; Ionov, D. S.; Anisimov, A. A.; Shchegolikhina, O. I.; Alfimov, M. V.; Muzafarov, A. M. Solvent-controlled intramolecular excimer emission from organosilicon derivatives of naphthalene. *Tetrahedron* **2021**, *93*, No. 132287.
- (7) Prigyi, N.; Channungkalakul, S.; Thanyalax, S.; Sukwattanasinit, M.; Ervithayasuporn, V. Cyclic siloxanes conjugated with fluorescent aromatic compounds as fluoride sensors. *Mater. Adv.* **2020**, *1*, 3358–3368.
- (8) Gou, Z.; Zhang, X.; Zuo, Y.; Tian, M.; Dong, B.; Lin, W. Pyrenyl-functionalized polysiloxane based on synergistic effect of highly selective and highly sensitive detection of 4-nitrotoluene. *ACS Appl. Mater. Interfaces* **2019**, *11*, 30218–30227.
- (9) Chairasert, T.; Channungkalakul, S.; Liu, Y.; Bureerug, T.; Silpcharu, K.; Unno, M.; Xiaogang, L.; Ervithayasuporn, V.; Chang,

Y.-T.; Rashatasakhon, P. Fluorescence Janus ring siloxanes for detection of Au(III) and L-cysteine. *Dyes Pigm.* **2022**, *208*, No. 110793.

(10) Pakhomov, A. A.; Kim, E. E.; Kononevich, Y. N.; Ionov, D. S.; Maksimova, M. A.; Khalchenia, V. B.; Maksimov, E. G.; Anisimov, A. A.; Shchegolikhina, O. I.; Martynov, V. I.; Muzafarov, A. M. Modulation of the photophysical properties of multi-BODIPY-siloxane conjugates by varying the number of fluorophores. *Dyes Pigm.* **2022**, *203*, No. 110371.

(11) Mohamed, M. G.; Kuo, S. W. Functional silica and carbon nanocomposites based on polybenzoxazines. *Macromol. Chem. Phys.* **2019**, *220*, No. 1800306.

(12) Mohamed, M. G.; Kuo, S.-W. Progress in the self-assembly of organic/inorganic polydendral oligomeric silsesquioxane (POSS) hybrids. *Soft Matter* **2022**, *18*, 5535–5561.

(13) Shirai, S.; Goto, Y.; Mizoshita, N.; Ohashi, M.; Tani, T.; Shimada, T.; Hyodo, S.-a.; Inagaki, S. Theoretical studies on Si-C bond cleavage in organosilane precursors during polycondensation to organosilica hybrids. *J. Phys. Chem. A* **2010**, *114*, 6047–6054.

(14) Ershova, T.; Anisimov, A.; Krylov, F.; Polschikova, N.; Temnikov, M.; Shchegolikhina, O.; Muzafarov, A. A new highly efficient method for the preparation of phenyl-containing siloxanes by condensation of phenylsilanols in liquid ammonia. *Chem. Eng. Sci.* **2022**, *247*, No. 116916.

(15) Kondo, S.-i.; Fukuda, A.; Yamamura, T.; Tanaka, R.; Unno, M. Anion recognition by a disiloxane-1,3-diol in organic solvents. *Tetrahedron Lett.* **2007**, *48*, 7946–7949.

(16) Kondo, S.-i.; Bie, Y.; Yamamura, M. Ratiometric fluorescence detection of anions by silanediol-based receptors bearing anthryl and pyrenyl groups. *Org. Lett.* **2013**, *15*, 520–523.

(17) Sato, Y.; Hayami, R.; Gunji, T. Characterization of NMR, IR, and Raman spectra for siloxanes and silsesquioxanes: a mini review. *J. Sol-Gel. Sci. Technol.* **2022**, *104*, 36–52.

(18) Masai, H.; Takahashi, M.; Tokuda, Y.; Yoko, T. Enhancement of polycondensation reaction by diethyl ether-aqueous NaOH immiscible two phase liquid treatment of phenyl-modified polysiloxane glass. *J. Ceramic Soc. Jpn.* **2005**, *113*, 259–262.

(19) Qing, G.; Cui, C. Controlled synthesis of cyclosiloxanes by NHC-catalyzed hydrolytic oxidation of dihydrosilanes. *Dalton Trans.* **2017**, *46*, 8746–8750.

(20) (a) Zimer, B.; Backer, M.; Auner, N. A triclinic polymorph of hexaphenylcyclotrisiloxane. *Acta Crystallogr., Sect. C: Cryst. Struct. Commun.* **1998**, *54*, 1111–11113. (b) Luo, M.; Yan, B. A simple synthesis of octaphenylcyclotetra(siloxane). *Tetrahedron Lett.* **2009**, *50*, 5208–5209.

(21) (a) Braga, D.; Zanotti, G. The room-temperature structure of octaphenylcyclotetra(siloxane). *Acta Crystallogr., Sect. B: Struct. Crystallogr. Cryst. Chem.* **1980**, *36*, 950–953. (b) Albright, A.; Gawley, R. E. NHC-catalyzed dehydrogenative self-coupling diphenylsilane: a facile synthesis of octaphenylcyclotetra(siloxane). *Tetrahedron Lett.* **2011**, *52*, 6130–6132.

(22) Cai, Y.; Samedov, K.; Dolinar, B. S.; Albright, H.; Guzei, I. A.; Hu, R.; Zhang, C.; West, R. Ring-shaped silafluorene derivatives as efficient solid-state UV-fluorophores: Synthesis, characterization, and photoluminescent properties. *Chem. - Eur. J.* **2014**, *20*, 14040–14050.

(23) Cai, Y.; Samedov, K.; Albright, H.; Dolinar, B. S.; Guzei, I. A.; Hu, R.; Zhang, C.; Tang, B. Z.; West, R. High solid-state fluorescence in ring-shaped AEE-active tetraphenylsilole derivatives. *Chem. Commun.* **2014**, *50*, 12714.

(24) Ganesan, P.; van Lagen, B.; Marcelis, A. T. M.; Sundöhlter, E. J. R.; Zuilhof, H. Siloxanes with pendent naphthalene diimides: Synthesis and fluorescence quenching. *Org. Lett.* **2007**, *9*, 2297–2300.

(25) Sun, R.; Feng, S.; Zhou, B.; Chen, Z.; Wang, D.; Liu, H. Flexible cyclosiloxane-linked fluorescent porous polymers for multifunctional chemical sensors. *ACS Macro Lett.* **2020**, *9*, 43–48.

(26) Imai, K.; Hatano, S.; Kimoto, A.; Abe, J.; Tamai, Y.; Nemoto, N. Optical and electronic properties of siloxane-bridged cyclic dimers with naphthylene or pyrenylene moieties. *Tetrahedron* **2010**, *66*, 8012–8017.

(27) Kondo, S.-i.; Taguchi, Y.; Bie, Y. Solvent dependent intramolecular excimer emission of di(1-pyrenyl)silane and di(1-pyrenyl)methane derivatives. *RSC Adv.* **2015**, *5*, 5846–5849.

(28) Grey, I. E.; Hardie, M. J.; Ness, T. J.; Raston, C. L. Octaphenylcyclotetrasiloxane confinement of C60 into double column arrays. *Chem. Commun.* **1999**, 1139–1140.

(29) Sheldrick, G. M. SHELXT—Integrated Space-Group and Crystal-Structure Determination. *Acta Crystallogr., Sect. A: Found. Adv.* **2015**, *71*, 3–8.

(30) Sheldrick, G. M. Crystal Structure Refinement with SHELXL. *Acta Crystallogr., Sect. C: Struct. Chem.* **2015**, *71*, 3–8.

(31) Frisch, M. J. et al. *Gaussian 16*, rev. A. 03; Gaussian Inc.: Wallingford, CT, 2016.